Jurnal Polimesin
Department of Mechanical Engineering
State Polytechnic of Lhokseumawe
http://e-jurnal.pnl.ac.id/polimesin
e-ISSN : 2549-1999 No. : 3 Month : June
p-ISSN : 1693-5462 Volume : 24 Year : 2026

Processing dates: received on 2025-12-1, reviewed on 2025-12-24, accepted on 2026-05-10 and online availability on 2026-06-30

Design optimization and material selection of automotive bushing arms using FEA under acidic exposure

Ana Nur Oktaviani[1], Dafit Feriyanto[1,*], Haftirman[1], Supaat Zakaria[2], Dedik Romahadi[1], Hadi Pranoto[1], SS Abdulmalik[3]
[1]Department of Mechanical Engineering, Universitas Mercu Buana, Jakarta 11650, Indonesia
[2]Politeknik Metro Johor Bahru, No 64, Jalan Suria 19, Taman Putera 81100, Johor Darul Takzim, Malaysia
[3]Department of Mechanical Engineering, Faculty of Engineering and Technology, Nigerian Army University, Biu, Nigeria
*Corresponding Author: dafit.feriyanto@mercubuana.ac.id

Abstract

Bushing arms are critical automotive components that function as vibration dampers and load absorbers. The problem is that the bushing arm often fails due to several factors, including the use of inappropriate materials, poor road quality, lack of routine maintenance, and external factors such as extreme temperatures, exposure to corrosion, and excessive pressure. This study aims to optimize bushing arm design and material selection to improve durability and vibration-damping performance under acidic exposure conditions. Two rubber materials, Natural Rubber (NR) and Ethylene-Propylene Diene Monomer (EPDM), were evaluated for MPV-type vehicle bushing arms. Three design variations were developed and analyzed using hyperelastic Finite Element Analysis (FEA) to assess stress distribution, strain, deformation, and safety factor. The rubber specimens were fabricated by hot pressing at 180°C and 7 MPa, followed by immersion in 15% phosphoric acid at 65°C to evaluate chemical degradation. Mechanical characterization included tensile testing (ASTM D412), Shore hardness testing, and microstructural observation. The results showed that acid immersion reduced tensile strength by 20.44% for NR and 23.80% for EPDM, while elongation decreased by 38.3% and 17.43%, respectively. Hardness decreased by 19.2% for NR and 4.81% for EPDM. FEA results indicated that design C achieved the lowest deformation, reducing it by 51%, while design B reduced shear stress and von Mises stress by up to 70%. Based on the combined mechanical and simulation results, design B with NR material was selected as the preferred configuration.

Keywords:
Bushing arm; accident; mechanical vibration; rubber; Finite Element Method

1 Introduction

The bushing arm is a vital component of the vehicle suspension system, responsible for connecting the control arm to the chassis and providing flexibility to absorb vibrations and maintain vehicle stability [1]. The bushing arm is equipped with rubber bearings (Fig. 1) that reduce vibration and noise transmitted from the road to the vehicle body, thereby enhancing driving comfort and safety [2]. Thus, the bushing arm is an integral part of the suspension system, balancing comfort, safety, and vehicle dynamics. However, its use often results in damage [3] that contributes to an increased risk of accidents. Data from large-scale used-car shows that approximately 30% of used vehicles exhibit detectable suspension faults, with worn or torn bushings being the most frequent culprit [3]. Symptoms of damage include vehicle imbalance, squeaking noises when driving over damaged roads, and declining suspension performance, which can increase the potential for accidents, especially at high speeds [4].

In real-world applications, bushing arms often fail due to various factors such as the use of inappropriate materials, poor road quality, and lack of routine maintenance. External factors such as extreme temperatures, exposure to corrosion, and excessive pressure on off-road vehicles also accelerate damage to this component [5][6]. Rubber materials commonly used in standard bushing arms provide good flexibility and vibration isolation but have limitations in wear resistance and high-temperature durability [6]. Therefore, selecting the appropriate material for the application requirements is crucial to improving bushing arm performance and service life [2]. Additionally, investigations into bushing arm failures indicate that suboptimal design and manufacturing processes can also exacerbate these problems [7].

A study related to bushing arms has been conducted by [8], which combines various parts designed to dampen shocks and vibrations. The results showed an average simulated cardanic stiffness value of 50.6 (Nm/°), torsional stiffness of 39.6 (Nm/°), axial stiffness of 23.6 (kN/mm), and radial stiffness of 75.6 (kN/mm). A 5% change in the design section decreased cardanic and torsional stiffness by 20% and radial stiffness by 15%.

A subsequent study developed an automated workflow to optimize rubber bushing design using Finite Element Analysis (FEA). This process involved parametric optimization for three-directional stiffness, followed by non-parametric shape optimization that increased fatigue life by 77% despite reducing stiffness. Further iterations with targeted stiffness produced an optimal design with a fatigue life 100% longer while maintaining appropriate stiffness [9].

Based on several previous studies, this research aims to design and optimize the material selection of bushing arms in MPV cars. Through this research, several new designs of bushing arms will be developed, which are expected to improve resistance to fatigue, loading, and abrasive properties compared to previous designs using the FEA method.

The research problems addressed are:

1. Rubber materials commonly used in bushing arms have limitations in terms of fatigue resistance, which can lead to accidents, loading, and abrasive environmental conditions that cause bushing arm failure.
2. The bushing arm design needs improvement through innovative designs to increase stiffness and optimal performance under maximum vehicle load conditions.
3. Modelling and simulation using FEA have become important for predicting bushing arm performance before manufacturing.

Therefore, the objectives of this research are:

1. Optimizing the selection of NR and Ethylene-Propylene Diene Monomer (EPDM) rubber materials through phosphoric acid soaking treatment, tensile testing, hardness testing, and microstructure testing to improve the performance and service life of the bushing arm.
2. Designing innovative bushing arms that not only meet rigidity requirements but also offer better durability and a higher safety factor compared to previous designs.
3. Using FEA simulation to evaluate the performance of bushing arm designs with various parameters, such as total deformation, equivalent stress, elastic strain, shear stress, safety factor, and lifetime, to produce optimal and efficient solutions.

The state of the art and novelty of this research lie in the integrative approach that combines a new bushing arm design, optimal rubber material selection (NR and EPDM), and FEA-based simulation analysis, which have rarely been implemented together

in previous studies. According to [9][10][11], FEA and material analysis have been utilized; however, those studies focused on a single aspect only, such as simulation or material characterization. In addition, the material in previous studies was not treated under acidic conditions. Other researchers were more focused on new designs and experimental testing without fully integrating both into a comprehensive simulation analysis approach [12][13][14]. This research offers novelty by combining material optimization, new design, and more in-depth FEA simulation to improve the durability and safety factor of rubber bushing arms. The phosphoric acid treatment will be conducted to simulate the real conditions of vehicle operation under various conditions, including wet or dry operating areas. Additionally, the emphasis on material testing through tensile and hardness tests as well as microstructure analysis provides a more complete perspective for developing more efficient and long-lasting design solutions.

2 Research methodology

2.1 Research process

The rubbers used in this study are Natural Rubber (NR) and EPDM. The preparation of research samples is adjusted according to the bushing arm manufacturing method being studied in collaboration with industry partners (Astra). Both NR and EPDM rubber materials are prepared to a thickness of 3 mm and cut into shore hardness test samples, namely 55 x 55 mm (made in 2 layers), and tensile test samples, 115 mm x 25 mm (in 1 layer). The NR and EPDM materials are processed by hot pressing at 180°C, 7 MPa pressure, and holding times of 10, 15, and 20 minutes for each side. Phosphoric acid (H_3PO_4) treatment is also applied to NR and EPDM materials, beginning with cleaning them using mild alkali or isopropyl alcohol. The concentration used for H_3PO_4 is 15% because it is an average condition between the lowest and the extreme condition, approximately 30%. Heating is then carried out at 65°C for 1, 1.5, and 2 hours. After this process, the samples are rinsed with deionized water and dried at room temperature.

2.2 Bushing arm design

The design engineering of the existing bushing arm and three new bushing arm designs was analyzed using ANSYS® software. The existing bushing arm available in the market is shown in Fig. 1.

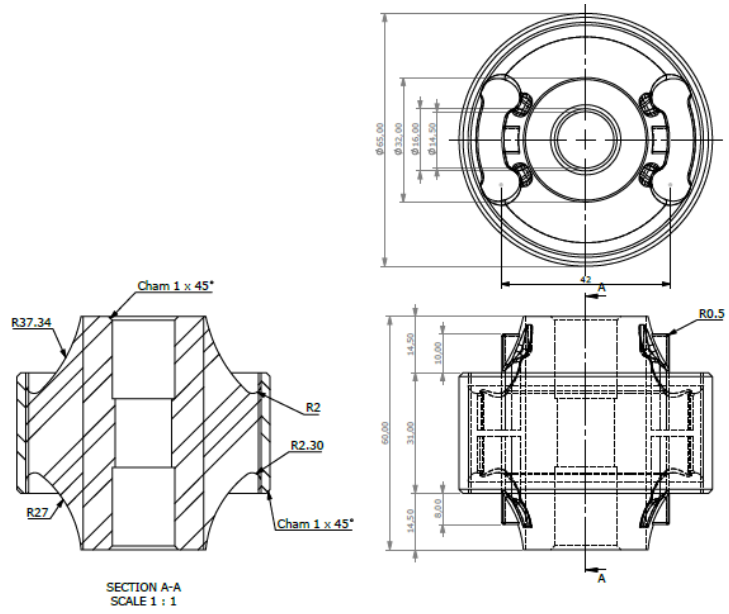

Fig. 1. Existing design of the bushing arm

The new design of the bushing arm refers to the previous initial design, but Design A (Fig. 2) is based on results of mounting design analysis according to [15], in which modifications were made by adding a radius to the rubber intended to absorb shocks on the bushing arm. The previous rubber radius sizes were 37.4 mm for the upper part and 27 mm for the lower part, and were later changed to 175 mm for the upper part and 136 mm for the lower part.

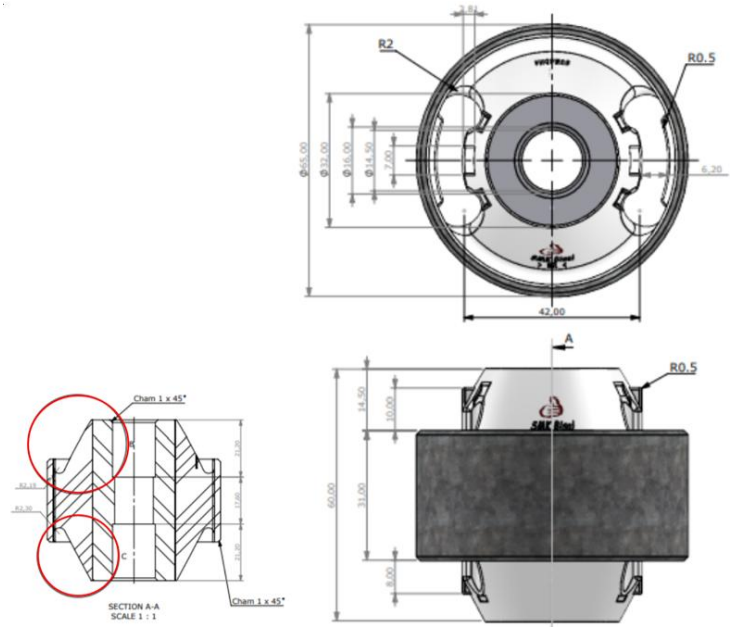

Fig. 2. Design A

In Design B (Fig. 3), the part marked with the letter B is made thinner than the initial design, from 2.89 mm to 2.11 mm, to reduce the stiffness value to achieve better damping. With reference to the results of previous design developments [16], this modification is intended to meet the stiffness requirements; however, it still presents critical areas around the hole in the bushing area, so further improvements are necessary in the subsequent design.

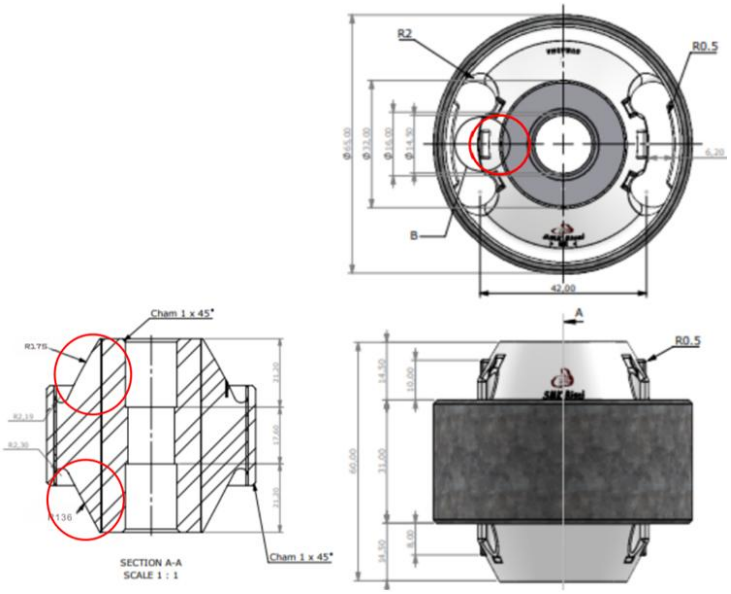

Fig. 3. Design B

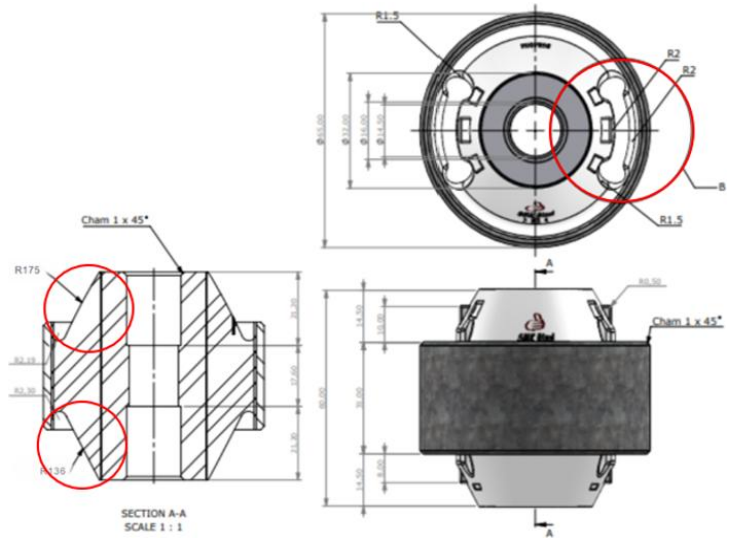

Fig. 4. Design C

Design C (Fig. 4) uses an offset by modifying the hole shape to be 1 mm smaller than before, aiming to reduce the stiffness value and achieve better damping properties. According to research findings [17], the radius size and contact distance of the bushing affect both the increase in stiffness and the magnitude of displacement in the bushing.

2.3 Analysis process

2.3.1 Tensile testing

Tensile testing is performed in accordance with ASTM D412 standards, which include: Method A uses dumbbell and straight-section specimens, while Method B uses cut ring-shaped specimens. Testing is based on ASTM D412 and is carried out using a universal testing machine at a speed of 500 ±50 mm/min and a tensile strength of 5 kN. There are 20 samples prepared for this analysis, consisting of 5 samples each for the various materials (NR and EPDM) and the treatment (without and with H_3PO_4). The requirements for preparing tensile test specimens are shown in Fig. 5.

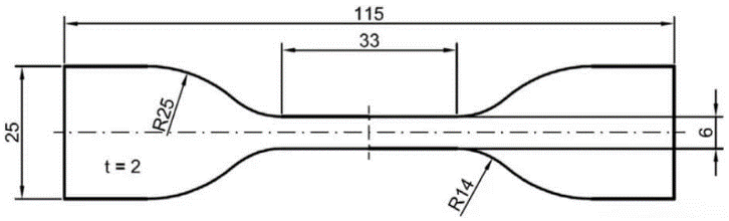

Fig. 5. ASTM D412 specimen dimensions

2.3.2 Microstructure

Microstructure testing using a microscope is used to identify vulcanization patterns, filler particles, or additive distribution in the rubber, observe micro-defects such as voids, inclusions, or microcracks, and assess the homogeneity of the rubber material. There are 4 samples prepared for this analysis, consisting of 2 NR samples with and without H_3PO_4 treatment and 2 EPDM samples with and without H_3PO_4 treatment. The equipment used is a metallurgical microscope, brand Meiji, type M7100, with magnifications of 25X, 50X, and 100X.

2.3.3 Simulation analysis

Geometry Modeling: Conducted using CAD software according to the specifications applicable to MPV vehicles. The geometry is exported to ANSYS® for further simulation.

Material Definition: The bushing arm material is entered into ANSYS® based on material data, such as elastic modulus, Poisson's ratio, and density.

Meshing: Performed to divide the model into small elements. Refinement is performed in critical areas such as joints to ensure the accuracy of stress and deformation distributions. The average element size ranges from 2 mm to 4 mm. Refinement or smaller dimensions are used around the center hole (bushing center). This is done to capture stress concentrations in greater detail in the area that will receive the shaft load.

Application of Loads and Boundary Conditions: Static and dynamic loads, as well as compressive loads, are applied to the bushing arm to simulate forces occurring during operation.

Simulation and Solution: The simulation is carried out using the FEA method to calculate stress, strain, deformation, and the safety factor. The simulation results are analyzed to see whether the stresses exceed the material's yield limit.

3 Results and discussion

3.1 Tensile strength analysis

3.1.1 NR material

The results of the tensile test on NR material with soaking treatment are shown in Fig. 6 and Fig. 7, indicating an average tensile strength of 7.67 MPa, which is lower than the untreated rubber condition (9.64 MPa), a reduction of about 20.44%. This phenomenon occurs due to the degradation of the rubber material during phosphoric acid soaking, which is abrasive in nature. Furthermore, the strain value of NR treated with phosphoric acid soaking also showed a reduction, from an average of 406.75% before treatment to 251% after soaking, amounting to a decrease of approximately 38.3%.

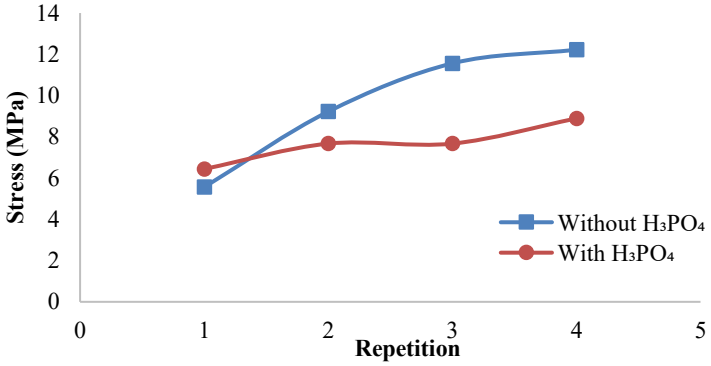

Fig. 6. Stress of the NR samples

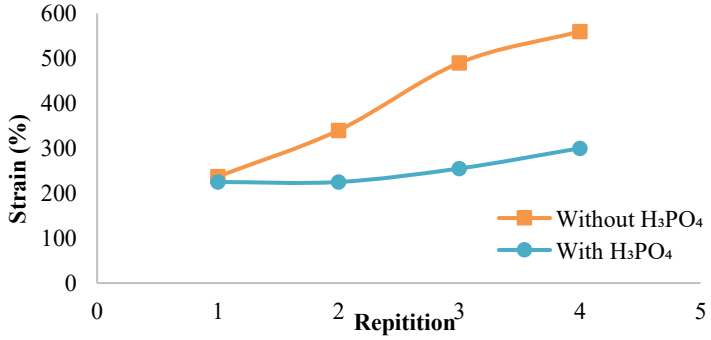

Fig. 7. Strain of the NR samples

In general, untreated rubber exhibits higher tensile strength, indicating that it can withstand greater tensile forces without deforming or failing. Moreover, according to [17, 18], in the context of vulcanized rubber, high tensile strength can indicate an optimal number of cross-links, thereby making the material stronger. For the first specimen without phosphate soaking, the value deviated from the trend due to its thinner thickness, resulting in a much lower tensile strength compared to the other specimens treated with phosphoric acid soaking.

3.1.2 EPDM material

The EPDM rubber's tensile test results (Fig. 8 and Fig. 9) indicated an average tensile strength decrease of 23.80%, dropping from 9.055 MPa before soaking to 6.9 MPa afterwards. Similarly, the average elongation of EPDM rubber declined by 17.43%, from 610% before immersion to 503.7% after immersion.

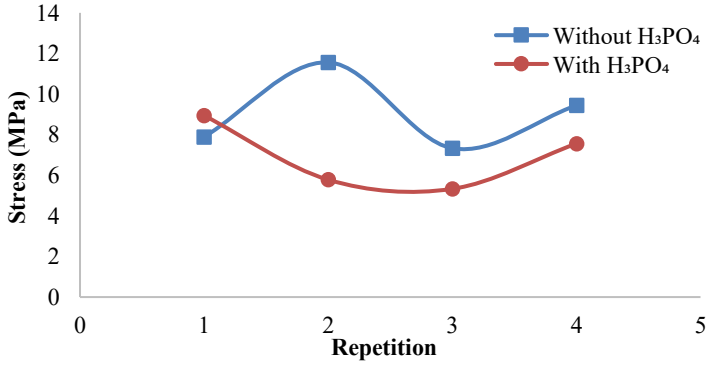

Fig. 8. Stress of the EPDM samples

Compared to NR rubber, EPDM demonstrates a higher reduction in tensile strength, yet its elongation values suggest better resilience. These observations imply that EPDM is softer and more flexible, but not as strong in resisting tensile loads. Phosphoric acid can function as a degrading agent, weakening the polymer networks in NR and EPDM by breaking cross-links within their molecular chains.

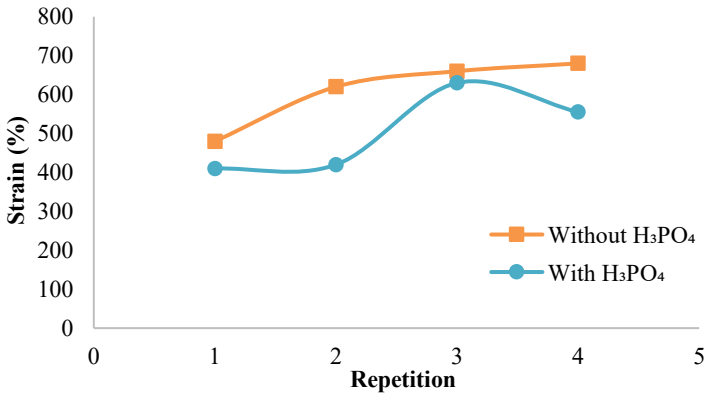

Fig. 9. Strain of the EPDM samples

This explains the reduction in tensile strength observed in both rubbers. However, EPDM's superior chemical resistance over NR means that its molecular structure is less affected by phosphoric acid. Still, extended exposure may result in changes to its physical and mechanical properties, particularly a reduction in tensile strength and resistance to stretching.

3.2 Microstructure analysis

The microstructure of NR (Fig. 10) exposed to phosphoric acid likely results in a reduction in cross-link density, as evidenced by the appearance of microcracks or a more loosely packed surface structure. Degradation induced by phosphoric acid can alter the surface morphology, making it more brittle and less homogeneous. Conversely, the microstructure of NR that has not been treated with phosphoric acid is likely denser and more organized, with stronger cross-links and a smoother surface, reflecting greater physical stability. In specimens subjected to immersion, the microstructure appears rougher with a less uniform particle distribution. The presence of visible fibers or pores indicates a structure that remains relatively intact, with no major signs of significant degradation [19]. Additionally, the surface seems denser and only slightly deformed, a result of the vulcanization process.

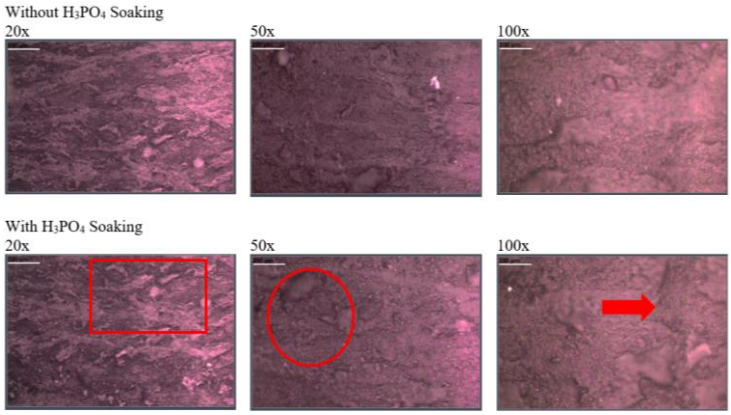

Fig. 10. Microstructure analysis of NR samples

Microstructure analysis of EPDM samples, as shown in Fig. 11. EPDM rubber immersed in phosphoric acid may show minor changes in its microstructure. However, due to its greater resistance to degradation, its structure generally remains stable, with only slight alterations in the surface layer or localized thinning. The microstructure of EPDM that is not affected by phosphoric acid tends to remain robust, displaying a homogeneous morphology and greater elasticity. This indicates that EPDM possesses superior resistance to degradation and retains its structural strength even without chemical treatment. According to [20], EPDM rubber has a denser and more uniform structure, as it can reduce the number of air voids as the content ratio increases.

If both rubbers are immersed in phosphoric acid, the effects will differ due to their distinct chemical properties and microstructures. For NR rubber, the microstructure deteriorates more quickly because its polymer chains are more reactive to chemical degradation. Tensile strength will drop significantly, as phosphoric acid weakens the cross-links within the NR polymer. The surface becomes rougher since the natural fibers in NR are more easily attacked by acid [21].

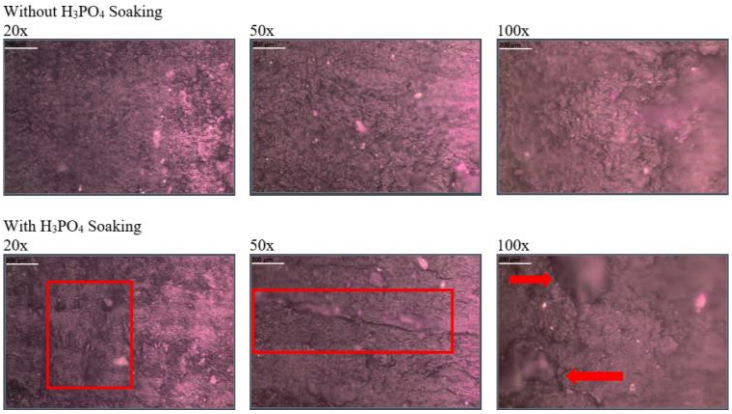

Fig. 11. Microstructure analysis of EPDM samples

EPDM rubber is more resistant to soaking in phosphoric acid because its structure is more chemically stable. Tensile strength remains relatively stable in the short term, though it may decrease if immersion is prolonged. The surface stays more homogeneous since EPDM's dense structure is not easily degraded by acid. Elongation changes are minimal, thanks to EPDM's superior thermal and chemical resistance compared to NR.

3.3 Simulation analysis

3.3.1 Deformation analysis

The deformation analysis of the existing design and various modified designs of the bushing arm is shown in Fig. 12. The Initial Design shows the highest deformation, especially for the EPDM material at 29.514 mm, while NR experiences deformation of 18.09 mm. After the design modification, deformation decreases across various design variations. Design A shows improvement with a total deformation of 16.339 mm for NR, representing a 9.7% decrease compared to the Initial Design. Meanwhile, EPDM in Design A undergoes deformation of 26.083 mm, indicating a reduction of 11.62%.

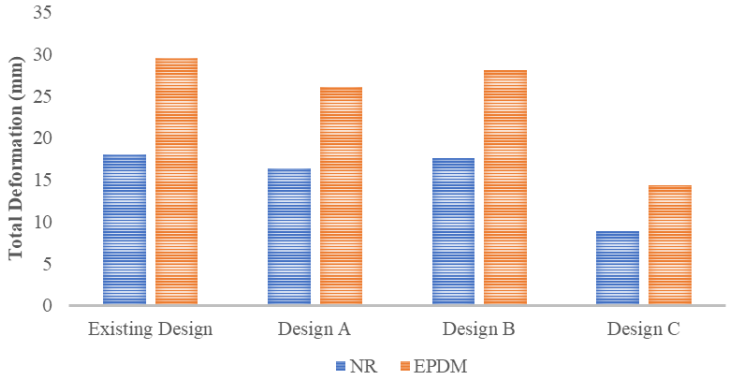

Fig. 12. Deformation analysis of the various bushing arm designs

Design B also shows improvement over the Initial Design, although not as effective as Design A. The NR material in this design exhibits deformation of 17.548 mm, a decrease of only about 3.9%. Meanwhile, the deformation in EPDM reaches 28.051 mm, a 5% reduction. Design C produces the smallest deformation among the designs. The NR material undergoes a deformation of 8.836 mm, resulting in a 51.08% reduction from the initial design. Meanwhile, EPDM undergoes a deformation of 14.358 mm, showing a decrease of 51.38%.

From these results, it can be concluded that Design C provides the most significant deformation reduction, more than 50% smaller than the Initial Design. This indicates that the geometric modification applied to Design C successfully increases the structural stiffness significantly, thereby reducing deformation under loading. According to [22] the initial static simulations for certain EPDM materials show total deformations exceeding 35 mm

when modeled with lower-order Ogden parameters. Another researcher [23] investigates the material behavior of the NR for the bushing arm, and the results show that the total shear deformation ranges from 100 mm to 200 mm.

3.3.2 Equivalent elastic strain analysis

The equivalent elastic strain analysis of the existing design and various modified designs of the bushing arm is shown in Fig. 13. The Initial Design represents the baseline configuration, exhibiting the highest levels of equivalent elastic strain for both types of elastomeric materials evaluated. Notably, EPDM recorded the maximum strain value of 5.8649 mm/mm, while NR demonstrated a lower, yet still substantial, strain of 3.6458 mm/mm under loading. These high strain levels indicate that, in its original form, the structure is particularly susceptible to elastic deformation, especially when utilizing EPDM as the constituent material.

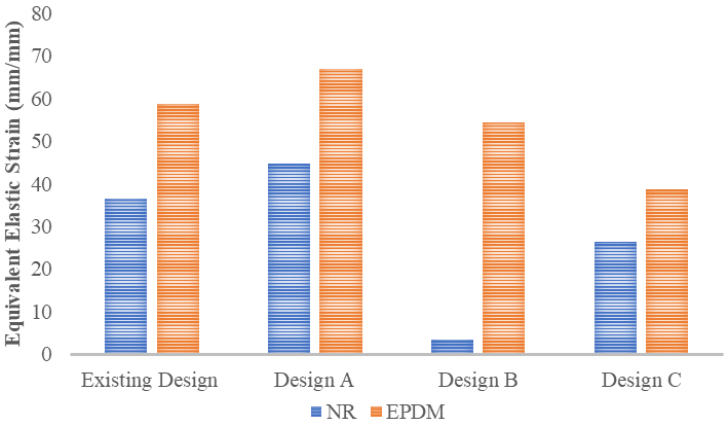

Fig. 13. Equivalent elastic strain analysis of the various bushing arm designs

Upon implementing design modifications, significant variations in strain response were observed across the three alternative design configurations (Design A, B, and C). Design A resulted in a decrease in equivalent elastic strain for NR, with strain reducing to 4.4632 mm/mm; this reflects an improvement of 22.4% compared to the Initial Design. However, for EPDM, the strain unexpectedly increased to 6.7052 mm/mm, a 14.3% increase. This indicates that Design A's geometric modifications are beneficial for NR but may inadvertently intensify strain when EPDM is used, potentially due to differences in the material's modulus or load distribution under the revised geometry.

Design B demonstrated a more balanced improvement for both materials. The equivalent elastic strain for NR decreased further to 3.443 mm/mm, indicating a modest 5.6% reduction relative to the Initial Design. Meanwhile, EPDM exhibited a decreased strain value of 5.4302 mm/mm, reflecting a 7.4% reduction. This suggests that Design B's modifications, while less effective for NR than for EPDM, were nonetheless able to reduce elastic deformation more consistently for both materials than Design A.

The most pronounced improvements were achieved with Design C. For NR, the equivalent elastic strain decreased sharply to 2.6334 mm/mm, representing a 27.8% reduction compared to the Initial Design. EPDM displayed a similarly significant improvement with strain reduced to 3.8756 mm/mm, a 33.9% decrease. Such findings indicate that the geometric changes implemented in Design C most effectively mitigate elastic deformation for both materials. The marked reduction in strain values highlights the superior effectiveness of this configuration in enhancing the stiffness and load-bearing capability of the structure.

In summary, the progressive refinement of design geometry had a clear impact on mitigating elastic strain, with Design C emerging as the most advantageous configuration. The reduction in elastic strain for both NR and EPDM in Design C signifies a notable improvement in structural integrity and resistance to deformation, making it a preferable solution for applications where high durability and reduced elastic deformation are critical. These results underscore the importance of tailoring geometrical modifications to accommodate specific material properties in order to optimize performance under service loads.

3.3.3 Maximum shear elastic strain analysis

The maximum shear elastic strain analysis of the existing design and various modified designs of the bushing arm is shown in Fig. 14. In the baseline (Initial Design), both EPDM and NR materials exhibited significant maximum shear elastic strains, with EPDM recording 9.771 mm/mm and NR recording 5.982 mm/mm. This high shear response reflects the susceptibility of both materials, especially EPDM, to deformation under shear loading conditions.

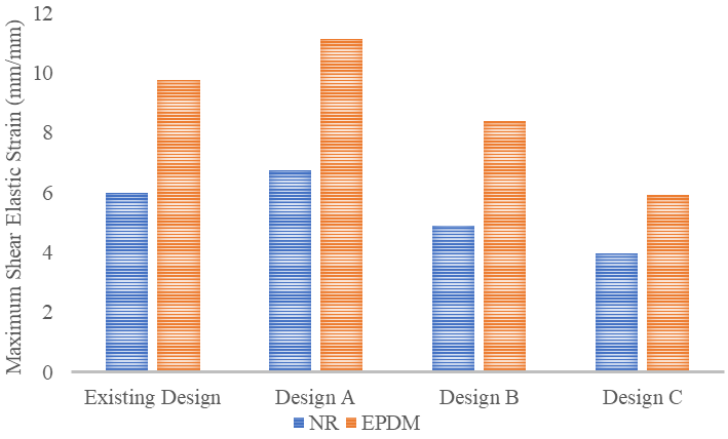

Fig. 14. Maximum shear elastic strain analysis of the various bushing arm designs

Subsequent design modifications produced notable differences in strain behavior between material types and configurations. Implementation of Design A resulted in increased maximum shear elastic strain values for both NR and EPDM, as evidenced by NR rising to 6.762 mm/mm (a 13% increase over the baseline), and EPDM elevating to 11.148 mm/mm (a 14.1% increase). These findings indicate that Design A's geometric features contributed to amplified shear deformation, suggesting the modifications were unfavorable for enhancing shear resistance.

In contrast, Design B presented a moderate improvement in shear characteristics. The maximum shear elastic strain of NR was reduced to 4.887 mm/mm, representing an 18.3% decrease from the Initial Design, while EPDM's strain was lowered to 8.389 mm/mm, corresponding to a 14.1% reduction. These reductions confirm the improved effectiveness of Design B in suppressing shear deformation, though the scale of improvement remained moderate.

The most substantial enhancement in shear resistance was achieved in Design C. Maximum shear elastic strain for NR declined dramatically to 3.964 mm/mm, a reduction of 33.7% compared to the Initial Design, while EPDM decreased to 5.914 mm/mm, achieving a reduction of 39.5%. The magnitude of these decreases demonstrates the superior efficacy of Design C's geometric configuration in mitigating shear deformation in both elastomeric materials.

In conclusion, Design C outperformed the other configurations with the most pronounced reductions in maximum shear elastic strain for both NR and EPDM. The effectiveness of Design C in reducing shear strain highlights the critical role of geometric optimization in enhancing the performance and durability of elastomeric materials subjected to shear loading.

3.3.4 Equivalent stress (Von-Mises) analysis

The equivalent stress (Von-Mises) analysis of the existing design and various modified designs of the bushing arm is shown in Fig. 15. The initial design exhibited equivalent stresses of 53.1 MPa for NR material and 48.82 MPa for EPDM. After the design modifications, variations in equivalent stress were observed. Design A showed a slight increase in stress compared to the initial design. For NR, the stress increased to 51.226 MPa, reflecting a

3.53% decrease from the original value. Meanwhile, for EPDM, the equivalent stress rose to 37.669 MPa, indicating a 22.8% reduction compared to the initial design.

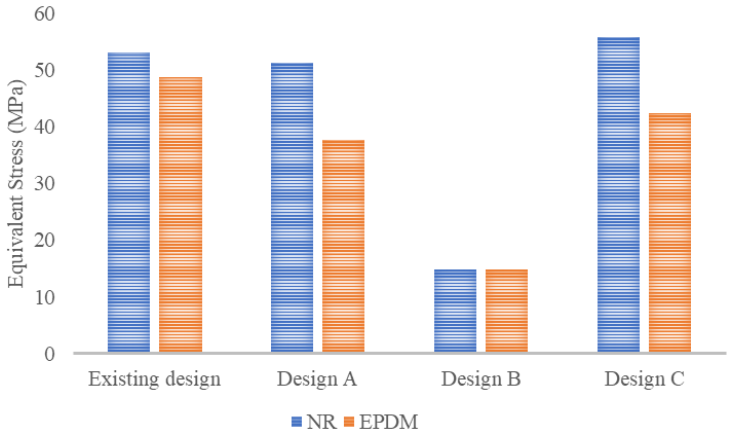

Fig. 15. Equivalent Stress (Von-Mises) analysis of the various bushing arm designs

Design B demonstrated a more significant stress reduction than Design A. The equivalent stress in NR decreased to 14.832 MPa, representing a 72.1% reduction, while in EPDM, it dropped to 14.804 MPa, a 69.7% reduction from the original design.

Design C produced a different outcome: for NR, the equivalent stress increased to 55.878 MPa (a 5.2% rise), whereas for EPDM, it declined to 42.369 MPa, a 13.2% reduction. Overall, Design B exhibited the best performance in reducing equivalent stress, achieving reductions of 72.1% for NR and 69.7% for EPDM. This indicates that Design B is the most effective configuration in minimizing the combined stress, thereby enhancing structural durability under applied loads.

3.3.5 Maximum shear stress analysis

The maximum shear stress analysis of the existing design and various modified designs of the bushing arm is shown in Fig. 16. The initial design recorded maximum shear stresses of 28.808 MPa for NR material and 26.016 MPa for EPDM. After implementing design modifications, variations in maximum shear stress values were observed. Design A exhibited a slight reduction compared to the initial design. For NR, the shear stress decreased to 28.12 MPa, representing a 2.4% reduction. For EPDM, the stress dropped to 20.349 MPa, indicating a 21.8% decrease.

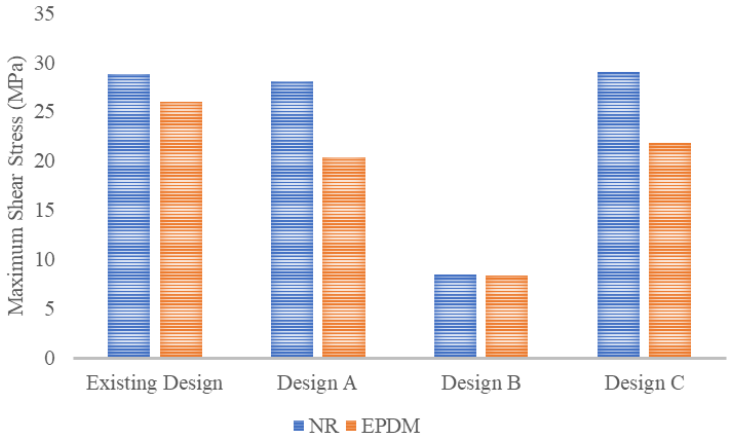

Fig. 16. Maximum Shear Stress analysis of the various bushing arm designs

Design B produced a more substantial reduction in shear stress than Design A. In NR, the maximum shear stress decreased to 8.427 MPa, marking a 70.8% reduction from the original design. In EPDM, it also dropped noticeably to 8.474 MPa, a reduction of 67.4%.

Design C showed a contrasting trend, with NR exhibiting an increase in maximum shear stress to 29.012 MPa, corresponding to a 0.7% rise. However, the EPDM material still showed a stress reduction to 21.789 MPa, a decrease of 16.2%. Overall, Design B demonstrated the best performance in reducing maximum shear stress, achieving substantial reductions of 70.8% for NR and 67.4% for EPDM. This indicates that Design B is the most efficient in mitigating shear loads on the materials, thereby enhancing the bushing arm's resistance to applied shear forces.

3.3.6 Safety factor analysis

The safety factor analysis of the existing design and various modified designs of the bushing arm is shown in Fig. 17. The initial design had a minimum safety factor of 3.484×10^{-6} for NR material and 5.838×10^{-7} for EPDM. In addition, the maximum safety factor is 2. Design A exhibited a slight improvement over the initial model, with values reaching 3.611×10^{-6} for NR (a 3.65% increase) and remaining at 5.083×10^{-7} for EPDM (a 12.95% decrease). However, some part of this design reaches the maximum safety factor of 5.

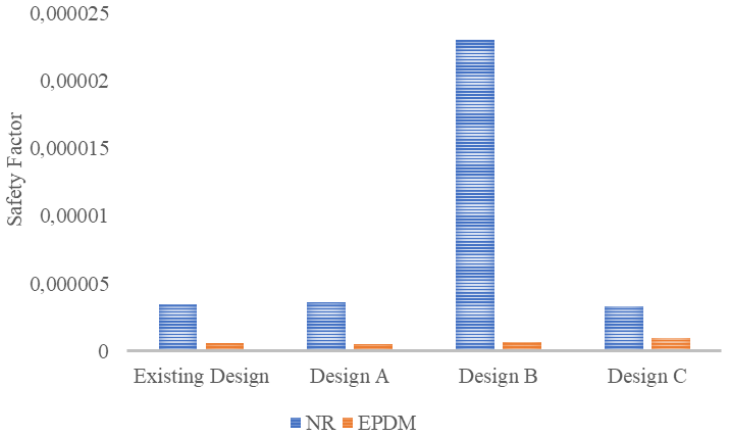

Fig. 17. Safety factor analysis of the various bushing arm designs

Design B demonstrated a significant improvement in the minimum safety factor. For NR, the value increased to 2.305×10^{-5}, representing a 561.6% rise, while for EPDM, it increased to 6.754×10^{-7}, or 15.68% higher than the initial design. However, some part of this design reaches the maximum safety factor of 5.

Design C yielded the greatest improvement for NR, with the minimum safety factor reaching 3.311×10^{-6}, an 81.5% increase from the initial value. For EPDM, the minimum safety factor also rose to 9.654×10^{-7}, marking a 65.43% increase. However, for maximum safety factor, it reaches 5.

Based on these findings, Design B provides the largest improvement in the safety factor for NR, with a 561.6% increase, indicating enhanced protection against potential failure. Conversely, Design C offers the greatest improvement for EPDM, with a 65.43% rise, signifying its effectiveness in enhancing material reliability. Despite these improvements, the minimum safety factor remains extremely low, indicating that certain regions still experience high stress concentrations, which could lead to premature structural failure. According to [24], which uses the Yeoh and Ogden models in FEA software to predict where cracks will initiate. They found that while NR is stronger, EPDM's life cycle is more predictable in high-heat environments where NR tends to become brittle.

4 Conclusions

This study evaluated the suitability of NR and EPDM rubber materials for automotive bushing arm applications through mechanical testing, acidic exposure, and FEA. Material selection was based on tensile performance and resistance to phosphoric acid to assess stability under aggressive conditions. The results showed that EPDM exhibited better mechanical stability after acid immersion, with lower reductions in hardness and elongation compared with NR, indicating better chemical resistance. However, both materials retained comparable initial mechanical performance. Based on dimensional requirements and functional considerations

for MPV-type vehicles, three refined bushing arm designs (A, B, and C) were developed and analyzed. Design C showed the lowest total deformation, improving by more than 50% compared with the original design, while design B reduced shear stress and von Mises stress by nearly 70%. NR exhibited a stiffer mechanical response, whereas EPDM showed greater elasticity with larger deformation. Considering the balance between structural stiffness and stress reduction, design B with NR material was identified as the most suitable configuration for bushing arm applications. Future work should address nonlinear rubber behavior, more representative loading conditions, and fatigue testing for improved simulation accuracy.

References

[1] D.B. Jebaraj, S.R. Prasanna, "Design and calculation of double arm suspension of a car. Journal of Mechanical Engineering, Automation and Control Systems," Vol. 1, No. 1, pp. 11–25, 2020.

[2] S. Taneva, H. Atanssov, K. Ambarev, S. Penchev, "Frequency Analysis of an Arm of Macpherson Suspension on a Passenger Car. Vide. Tehnologija," Resursi - Environment, Technology, Resources, Vol. 3, pp. 252–256, 2023.

[3] J.Y.J.T.Y.J.D. Bang, "Accelerated Life Testing Data-Based Lifetime Prediction of Rubber Material for Bushing Using Global-Local Optimization Technique," Journal of Applied Reliability, Vol. 23, pp. 211–220, 2023.

[4] Deng, S. Xue, R. Guo, "Failure Analysis of an Automotive Bushing," Journal of Failure Analysis and Prevention, Vol. 18, No. 6, pp. 1379–1385, 2018.

[5] Cernuda, I. Llavori, A.C. Zăvoianu, A. Aguirre, A. Zabala, J. Plaza, "Critical Analysis of the Suitability of Surrogate Models for Finite Element Method Application in Catalog-Based Suspension Bushing Design," IEEE International Conference on Emerging Technologies and Factory Automation, pp. 829–836, 2020.

[6] Z.J. Liu, Q. Bi, J. Guo, G. Liu, M. Zhou, H. Qingxue, "Failure analysis of eccentric bushings in large gyratory crusher," Engineering Failure Analysis, Vol. 153, p. 107630, 2023.

[7] Y. Qian, W. Huang, D. Li, H. Zhang, P. Liu, Z. Peng, "Optimization design of bushing of distribution switchgear equipment," IEEE International Conference on High Voltage Engineering and Application, pp. 1-4, 2016.

[8] Nasruddin, T. Susanto, "Study of the mechanical properties of natural rubber composites with synthetic rubber using used cooking oil as a softener," Indonesian Journal of Chemistry, Vol. 20, No. 5, pp. 967–978, 2020.

[9] W. Kang, J. Liu, W. Xiong, T. You, X. Wang, K. Zeng, Y. Deng, Z. Guo, K. Yuan, "Basic mechanical and fatigue properties of rubber materials and components for railway vehicles: A literature survey," Reviews on Advanced Materials Science, Vol. 61, No. 1, pp. 587–610, 2022.

[10] N. Nasruddin, A.T. Bondan, "Efek Penambahan Epdm Pada Karet Alam Terhadap Sifat Mekanik Karet Busa," Jurnal Dinamika Penelitian Industri, Vol. 29, No. 2, p. 155, 2018.

[11] Supriyono, T. Mulyanto, M.D. Ardiyan, "Penelitian Sifat Mekanik Baja Karbon ST41 Hasil Reduksi pada Mesin Roll Datar," Jurnal Teknik FTUP, Vol. 28, No. 2, pp. 71–78, 2015.

[12] L. Teixeira, B.D.R. Pereira, T.G. Bortoly, J.A. Brancher, O.M. Tanaka, O. Guariza-Filho, "The environmental influence of light coke™, phosphoric acid, and citric acid on elastomeric chains," Journal of Contemporary Dental Practice, Vol. 9, No. 7, pp. 017–024, 2008.

[13] J. Rivas-Torres, J.C. Tudon-Martinez, J.D.J. Lozoya-Santos, R.A. Ramirez-Mendoza, A. Spaggiari, "Analytical design and optimization of an automotive rubber bushing," Shock and Vibration, pp. 1-13, 2019.

[14] R. Pornprasit, P. Pornprasit, P. Boonma, J. Natwichai, "Determination of the mechanical properties of rubber by FT-NIR," Journal of Spectroscopy, No. 1, pp. 1-7, 2016.

[15] C.S. Woo, H.S. Park, K.S. Kim, J.H. Choi, "Useful life time evaluation and prediction for automotive rubber mount," 19th European Conference on Fracture: Fracture Mechanics for Durability, Reliability and Safety, pp. 1-7, 2012.

[16] Henri, "Pengertian Karet Gelang," Angewandte Chemie International Edition, Vol. 6, No. 11, pp. 951–952, 2018.

[17] M.N.H. Pasaribu, M. Sabri, I. Nasution, "Analisa Koefisien Gesek Kinetis Terhadap Struktur Permukaan Jalan Akibat Beban Dinamik Mobil," Talenta Conference Series: Energy and Engineering (EE), Vol. 1, No. 1, pp. 047–051, 2018.

[18] D. Feriyanto, Z. Zaenudin, "Innovative catalytic converter from FeCrAl material coated by γ-Al2O3 and NiCr for increasing thermal stability at high temperature operation," Jurnal Polimesin, Vol. 21, No. 6, pp. 636-640, 2023

[19] D. Feriyanto, S. Zakaria, H. Pranoto, S.E. Pratiwi, M. Fitri, I. Hidayat, "Coating Thickness Analysis Of Electroplated Fecral Material For Catalytic Converter Application," Resmilitaris, Vol. 12, No. 4, pp. 1620-1628, 2022.

[20] H. Pranoto, A.M. Leman, D. Feriyanto, A. Adriansyah, A Wahab, "The innovative design of automatic speed limiter device for trucks and buses based on road location analysis," SINERGI, Vol. 26, No. 1, pp. 1-22, 2022

[21] D. Feriyanto, S.S.A. Malik, M. Fitri, I. Hidayat, H. Pranoto, S. Zakaria, "Effect of Material Composition on Thermal Stability Analysis of Coated and Uncoated FeCrAl CATCO by Î³-Al2O3 Ultrasonic-Electroplating Technique," Journal of Sustainable Materials Processing and Management, Vol. 1, No. 1, pp. 1-7, 2021

[22] H. I. Moon, H. G. Kim, and S. G. Kim, "Fatigue life prediction of EPDM rubber bushing," *Transaction of the Korean Society of Automotive Engineers*, vol. 19, no. 1, pp. 110–118, Jan. 2011.

[23] A. Naeem and H. K. Kim, "Numerical simulation of natural rubber bearing," in *Proceedings of the 2018 International Conference on Computing, Mathematics and Engineering Technologies (iCoMET)*, Sukkur, Pakistan, 2018, pp. 1–6.

[24] X. Qiu, H. Yin, and Q. Xing, "Research Progress on Fatigue Life of Rubber Materials," *Polymers*, vol. 14, no. 21, p. 4592, Oct. 2022